

TITLE
*ASP Conference Series, Vol. **VOLUME***, **PUBLICATION YEAR**
 EDITORS

Radiative cooling in SPH hydrodynamical simulations of X-ray clusters

R. Valdarnini

SISSA Via Beirut 2-4 34014, Trieste, Italy

Abstract. The results from hydrodynamical TREESPH simulations of galaxy clusters are used to investigate the dependence of the final cluster X-ray properties upon the numerical resolution and the assumed star formation models for the cooled gas. When cold gas particles are allowed to convert into stars the final gas profiles show a well defined core radius and the temperature profiles are nearly flat. Star formation methods based on a local density threshold, as in Navarro and White (1993), are shown to give stable results. Final X-ray luminosities are found to be numerically stable, with uncertainties of a factor ~ 2 .

1. Introduction

Hydrodynamical simulations have been widely used to predict for different theoretical frameworks the time evolution of the temperature distribution of X-ray clusters. With increasing availability of computational power numerical hydrodynamical simulations have been attempted to model the effects of radiative cooling on the gas in the formation and evolution of cluster galaxies (Katz & White 1993; Anninos & Norman 1996; Yoshikawa, Jing & Suto 2000; Pearce et al. 2000; Lewis et al. 2000). In this contribution I will show the preliminary results that have been obtained from a series of hydrodynamical SPH simulations of galaxy clusters. The simulations have different numerical resolution and include the effects on the gas component of radiative losses, star formation and energy feedback from SN. Final profiles are compared in order to assess the effects of numerical resolution, or different star formation prescriptions, on the cluster X-ray variables.

2. Simulations

In a previous paper (Valdarnini et al. 1999, hereafter VGB) a large set of hydrodynamical simulations was used to study the global X-ray cluster morphology and its evolution. The simulations were run using a TREESPH code with no gas cooling or heating. I refer to VGB for a detailed description of the simulations. In Valdarnini (2001) I have used the same cluster sample to study the effects of including in the simulations additional physics such as gas cooling and star formation. I will report here the results for the cluster with label Λ CDM00 in VGB. This is the most massive cluster ($M_v \simeq 1.5 \cdot 10^{15} M_\odot$) extracted from a cosmological Λ CDM N-body simulation with size $L = 200h^{-1} Mpc$, matter den-

sity $\Omega_m = 0.3$ and Hubble constant $H_0 = 70 \text{ Km sec}^{-1} \text{ Mpc}^{-1}$. In order to check the effects of radiative cooling for this cluster a set of TREESPH simulations was performed, with initial conditions provided by the cosmological simulation. The effects of radiative cooling are modelled in these simulations by adding to the SPH thermal energy equation an energy-sink term represented by the radiative cooling function. The simulation parameters are: number of gas particles, $N_g \sim 22,500$; gas particle softening parameter $\epsilon_g \sim 30 \text{ Kpc}$; gas particle mass, $m_g \sim 10^{10} M_\odot$; number of dark particles, $N_d \sim 45,000$ (including those in an external shell surrounding the cluster, cf. VGB).

Allowing the gas to cool radiatively will produce dense clumps of gas at low temperatures ($\simeq 10^4 \text{ K}$). In these regions the gas will be thermally unstable and will likely meet the physical conditions to form stars. In TREESPH simulations star formation (SF) processes have been implemented using different approaches. According to Katz, Weinberg & Hernquist (1996, hereafter KWH) a gas particle is in a star forming region if the flow is convergent and the local sound crossing time is larger than the dynamical time (i.e. the fluid is Jeans unstable). In a simplified version Navarro & White (1993, hereafter NW) assume as a sufficient condition that a gas particle must be in a convergent flow and its density exceeds a threshold ($\rho_g > \rho_{g,c} = 7 \cdot 10^{-26} \text{ g cm}^{-3}$). If a gas particle meets these criteria then it is selected as an eligible particle to form stars. The local star formation rate (SFR) obeys the equation

$$d\rho_g/dt = -c_\star \rho_g / \tau_g = -d\rho_\star/dt, \quad (1)$$

where ρ_g is the gas density, ρ_\star is the star density, c_\star is a characteristic dimensionless efficiency parameter, τ_g is the local collapse time and it is the maximum of the local cooling time τ_c and the dynamical time τ_d . At each step the probability that a gas particle will form stars in a time step Δt is compared with a uniform random number. If the test is successful then a mass fraction ε_\star of the gas mass is converted into a new collisionless particle. This star particle has the position, velocity and gravitational softening of the original gas particle. Typical assumed values are $\varepsilon_\star = 1/3$ and $c_\star = 0.1$ (KWH). For the local SFR, NW adopt Eq. 1 with $c_\star = 1$, $\tau_g = \tau_d$ and $\varepsilon_\star = 1/2$ when a gas particle can convert part of its mass into a star particle. The numerical tests have been performed following the NW prescriptions for selecting gas particles which can form stars. Once a star particle is created it can release energy into the surrounding gas through supernova (SN) explosions. All the stars with mass above $8 M_\odot$ end as a SN, leaving a $1.4 M_\odot$ remnant. The SN energy ($\simeq 10^{51} \text{ erg}$) is released gradually into the gas according to the lifetime of stars of different masses.

3. Results

Three simulations were performed with the same numerical parameters, but using different SF methods or parameters. This in order to test the final dependence of the cluster X-ray variables on the assumed star formation model for the cooled gas. In simulation I cold gas particles have been converted into stars according to the NW method. In the other two runs (II and III) the KWH prescription is adopted for converting gas particles into stars, but with different values of the star formation efficiency parameter c_\star : 0.1 and 1.. As is shown in

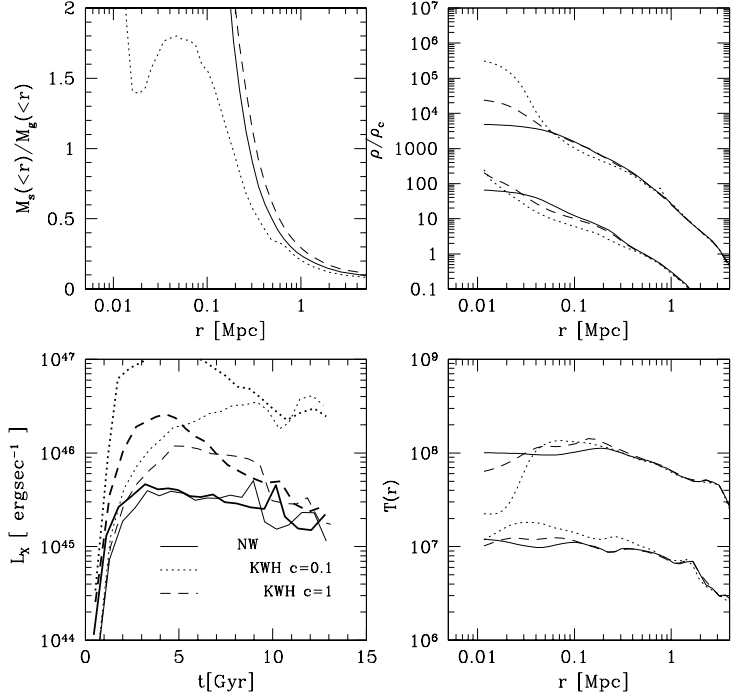


Figure 1. Plots showing several cluster properties in simulation runs with different SF prescriptions. The continuous line refers to the NW method, the others to KWH with different c_* (c in the bottom left panel). *Top left*: ratio of the star mass within the radius r over the gas mass within r . *Top right*: final radial density behavior for the gas component. The simulation results are compared with the corresponding high-resolution runs (see text). To facilitate a comparison the radial profiles of the high resolution results have been shifted downward by 10^k , $k = 2$ for densities and $k = 1$ for temperatures. *Bottom right*: Radial temperature profiles. *Bottom left* : X-ray luminosity versus time, the thick lines correspond to the high resolution simulations.

Fig. 1 the most important differences are found between the KWH simulations with different c_* . The differences are dramatic in the final X-ray luminosities, which differ by a factor $\simeq 40$. The source of this discrepancy relies in the different gas density profiles, which have substantial differences in the cluster core regions for $r \lesssim 100Kpc$. These differences are localized at the cluster center, beyond $r \simeq 100Kpc$ all the profiles converge, as it is shown in the plots of Fig. 1. The temperature profiles have a peak value of $\simeq 10^8 K$ at $r \simeq 100Kpc$ and thereafter decline outward by a factor ~ 2 out to r_v . Below $\sim 100Kpc$ the profiles instead show large differences. Compared to the NW run the simulation with $c_* = 0.1$ has gas temperatures which decline inwards by a factor ~ 10 from $\sim 100Kpc$ down to $r \sim 10Kpc$. These radial decays follow because of the less efficient conversion of the cooled gas into stars compared to the NW run. There is a remarkable agreement for the ratio of cluster mass locked into stars to the gas mass, which is $\simeq 10\%$ at r_v for all the runs considered. In order to assess the effects of numerical resolution upon final results simulations I, II and III have been run again but with a number of particles increased by a factor $\simeq 3$. These simulations will be referred as IH, IIH and IIIH, respectively. The simulation results are shown in Fig. 1. For simulations IH there are not appreciable differences in the radial profiles. The profiles of simulation IIH are instead different from those of run II at $r \lesssim 50Kpc$. The strong drop in $T(r)$ has been removed and the gas density profile is much closer to the NW one. Simulation IIIH yields final profiles very similar to the ones of the parent simulation. The bottom left panel of Fig. 1 shows that high resolution runs have final X-ray luminosities which can differ within a factor ~ 2 from the parent simulations.

To summarize, the above results demonstrate that simulations I and III have an adequate numerical resolution to reliably predict X-ray cluster properties, such as the X-ray luminosity. For simulation II (KWH with $c_* = 0.1$) there are large differences at the cluster core between the final profiles when the numerical resolution is increased.

References

Anninos, P. & Norman, M.L. 1996, ApJ, 459, 12
 Katz, N. & White, S.D.M. 1993, ApJ, 412, 455
 Katz, N., Weinberg, D.H. & Hernquist, L. 1996, ApJS, 105, 19
 Lewis, G.F., Babul, A., Katz, N., Quinn, T., Hernquist, L. & Weinberg, D.H. 2000, ApJ 536, 623
 Navarro, J. & White, S.D.M. 1993, MNRAS, 265, 271 (NW)
 Navarro, J., Frenk C.S. & White, S.D.M. 1995, MNRAS, 275, 720
 Pearce, F.R., Thomas, P.A., Couchman, H.M.P. & Edge, A.C. 2000, MNRAS 317, 1029
 Valdarnini, R., Ghizzardi, S. & Bonometto, S. 1999, New Astr, 4, 71 (VGB)
 Valdarnini, R. 2001, ApJ, in press
 Yoshikawa, K., Jing, Y.P. & Suto, Y. 2000, ApJ, 535, 593 (YJS)